NeuroImage: Clinical 37 (2023) 103322

Contents lists available at ScienceDirect

NeuroImage: Clinical

journal homepage: www.elsevier.com/locate/ynicl

Molecular imaging of the association between serotonin degeneration and beta-amyloid deposition in mild cognitive impairment

Gwenn S. Smith [a,b,*], Hillary Protas [c], Hiroto Kuwabara [b], Alena Savonenko [d], Najlla Nassery [e], Neda F. Gould [a], Michael Kraut [f], Dimitri Avramopoulos [g], Daniel Holt [b], Robert F. Dannals [b], Ayon Nandi [b], Yi Su [c], Eric M. Reiman [c], Kewei Chen [c]

[a] Division of Geriatric Psychiatry and Neuropsychiatry, Department of Psychiatry and Behavioral Sciences, Johns Hopkins University School of Medicine, Baltimore, MD, USA
[b] Division of Nuclear Medicine and Molecular Imaging, Russell H. Morgan Department of Radiology and Radiological Sciences, Johns Hopkins University School of Medicine, Baltimore, MD, USA
[c] Banner Alzheimer's Institute, Phoenix, AZ, USA
[d] Department of Pathology (Neuropathology), Johns Hopkins University School of Medicine, Baltimore, MD, USA
[e] Division of General Internal Medicine, Department of Medicine, Johns Hopkins University School of Medicine, Baltimore, MD, USA
[f] Division of Neuroradiology, Russell H. Morgan Department of Radiology and Radiological Sciences, Johns Hopkins University School of Medicine, Baltimore, MD, USA
[g] Department of Genetic Medicine, Johns Hopkins University School of Medicine, Baltimore, MD, USA

A B S T R A C T

Background: Degeneration of the serotonin system has been observed in Alzheimer's disease (AD) and in mild cognitive impairment (MCI). In transgenic amyloid mouse models, serotonin degeneration is detected prior to widespread cortical beta-amyloid (Aβ) deposition, also suggesting that serotonin degeneration may be observed in preclinical AD.

Methods: The differences in the distribution of serotonin degeneration (reflected by the loss of the serotonin transporter, 5-HTT) relative to Aβ deposition was measured with positron emission tomography in a group of individuals with MCI and a group of healthy older adults. A multi-modal partial least squares (mmPLS) algorithm was applied to identify the spatial covariance pattern between 5-HTT availability and Aβ deposition.

Results: Forty-five individuals with MCI and 35 healthy older adults were studied, 22 and 27 of whom were included in the analyses who were "amyloid positive" and "amyloid negative", respectively. A pattern of lower cortical, subcortical and limbic 5-HTT availability and higher cortical Aβ deposition distinguished the MCI from the healthy older control participants. Greater expression of this pattern was correlated with greater deficits in memory and executive function in the MCI group, not in the control group.

Conclusion: A spatial covariance pattern of lower 5-HTT availability and Aβ deposition was observed to a greater extent in an MCI group relative to a control group and was associated with cognitive impairment in the MCI group. The results support the application of mmPLS to understand the neurochemical changes associated with Aβ deposition in the course of preclinical AD.

1. Introduction

Molecular imaging methods, used to visualize and to quantify the neuropathology of Alzheimer's disease (AD) *in vivo,* provide an unprecedented opportunity to understand the neurobiology of preclinical AD. With these neuroimaging methods, mechanistic hypotheses that are based on data from human neuropathology and transgenic AD mouse models can be tested in the living human brain. These methods can be applied uniquely to obtain a fuller understanding of the neurobiological mechanisms associated with mild cognitive impairment (MCI) and its clinical progression to AD in order to identify targets for prevention and treatment. Beta-amyloid (Aβ) and Tau studied using positron emission tomography (PET) show associations with cognitive deficits and cognitive decline that are enhanced by including measures in statistical models that are associated with neurodegeneration, such as brain structure (gray matter volumes) or brain function (cerebral glucose metabolism/cerebral blood flow; Brier et al., 2016; Engler et al., 2006; Jack et al., 2009; Jagust, 2016; Mormino et al., 2009; Insel et al., 2017).

* Corresponding author at: Richman Family Professor of Alzheimer's Disease and Related Disorders, Division of Geriatric Psychiatry and Neuropsychiatry, Department of Psychiatry and Behavioral Sciences, Johns Hopkins University School of Medicine, Johns Hopkins Bayview Medical Center, 5300 Alpha Commons Drive, 4th floor, Baltimore, MD 21224.
E-mail address: gsmith95@jhmi.edu (G.S. Smith).

https://doi.org/10.1016/j.nicl.2023.103322
Received 1 June 2022; Received in revised form 28 December 2022; Accepted 5 January 2023
Available online 6 January 2023

Further, in AD patients, clinical progression despite brain clearance of Aβ by immunization, further highlights the importance of understanding aspects of neurodegeneration associated with Aβ deposition (Holmes et al., 2008; Salloway et al., 2014). Thus, studying more specific aspects of neurodegeneration may be informative.

Of the molecular mechanisms potentially associated with Aβ, strong evidence supports the investigation of the serotonin system in the preclinical stages of AD. Serotonin plays a significant role in normal brain function and modulates fundamental behaviors, including mood, sleep, appetite and cognition that are affected in preclinical AD (Lucki, 1998). The critical role of serotonin in the central nervous system is underscored by the dense serotonin innervation, as every cortical cell in the rat brain is in close proximity to a serotonin-containing neuron. (Molliver, 1987; Steinbusch et al., 1981). The localization of the serotonin transporter (5-HTT) suggests its important modulatory role in cortical, limbic and sub-cortical circuits affected in preclinical AD. Human postmortem autoradiography shows high 5-HTT binding in anterior and subcallosal cingulate, entorhinal and insular cortices, temporal pole, hippocampal formation, medial caudate, putamen, ventral striatum, thalamus (anterior, mediodorsal and pulvinar nuclei) and raphe nuclei (Varnäs et al., 2004). Vulnerability of cortical serotonin projections is observed in neuropathology and neuroimaging studies in AD, as well as in transgenic amyloid mouse models (Bowen et al., 1983; Hirao et al., 2015; Liu et al., 2008). Importantly, preclinical evidence supports the use of treatments targeting the serotonin system based on its multiple neurochemical and molecular effects relevant to prevention and symptomatic treatment of both cognitive deficits and neuropsychiatric symptoms (Ramirez et al., 2014). Thus, the serotonin system may represent a promising, therapeutic target.

Among the earliest neuropathological changes observed in AD, before widespread cortical distribution of AD pathology (Aβ and Tau), is AD pathology and cell loss in the serotonergic cell bodies of origin (raphe nuclei) of cortical projections (Curcio and Kemper, 1984; Mann and Yates, 1983; Rüb et al., 2000, 2016; Simic et al., 2009; Grinberg et al., 2009). Serotonin degeneration is more widespread than other neurotransmitter deficits in AD and is correlated to a greater extent with cognitive decline than degeneration of other monoaminergic and cholinergic systems (Garcia-Alloza et al., 2004; Lyness et al., 2003). Molecular imaging studies have observed serotonin degeneration in MCI and AD. In AD patients, relative to healthy controls, lower striatal 5-HTT and lower cortical 5-HT1A and 5-HT2A receptors have been reported (Blin et al., 1993; Kepe et al., 2006; Ouchi et al., 2009). Higher cortical and hippocampal 5-HT4 availability is associated with greater Aβ deposition and correlated with global cognitive impairment in AD patients (Madsen et al., 2011) In MCI relative to controls, lower cortical and limbic 5-HTT has been reported that was correlated with greater deficits in auditory-verbal and visual-spatial memory in the MCI, not the control group (Smith et al., 2017). Further, lower cortical and higher hippocampal 5-HT1A receptors and lower cortical 5-HT2A receptors have been reported in MCIs relative to controls (Kepe et al., 2006; Truchot et al., 2007; Hasselbalch et al., 2008). Lower 5-HT1A receptors were correlated with greater global cognitive deficits, whereas lower 5-HT2A receptors were correlated with greater neuropsychiatric symptoms, not with greater cognitive deficits (Kepe et al., 2006; Hasselbalch et al., 2008). While 5-HT2A receptors were reduced in MCI compared to controls, 5-HT2A receptors were relatively stable at two year follow-up, despite progression to AD in over 50 % of MCI participants (Marner et al., 2011). Preliminary data show longitudinal decreases in 5-HTT in MCI (Smith, et. al., unpublished data). Thus, 5-HTT may be more sensitive to cognitive deficits and cognitive decline than serotonin receptors. Cortical regions that show a loss of serotonin enervation overlap with regions that show cortical Aβ deposition. Serotonin degeneration, either preceding Aβ deposition or as a downstream event, may be involved in the transition from MCI to AD.

Several lines of evidence show an association between serotonin degeneration and Aβ deposition . In transgenic Aβ mouse models (APPswe/PS1dE9), significant reductions in cortical and hippocampal serotonin fiber densities were observed at the onset of deficits in episodic memory (12 months), before widespread Aβ deposition (18-24 months), suggesting that serotonin degeneration may be an early event associated with Aβ deposition (Liu et al., 2008). At the onset of reference memory deficits and anxiety symptoms (18 months), there was a further decline in cortical serotonin fiber densities and loss of serotonin neurons in the raphe nucleus. In contrast, a relative preservation of cholinergic efferents and cell bodies and modest cortical and hippocampal neuronal loss was observed. Further studies in the sametransgenic Aβ mouse model showed a loss of 5-HTT and 5-HT1b receptors and decreased serotonin release that was associated with an increase in the Aβ-related inflammatory response (Metaxas et al., 2019; Tajeddinn et al., 2015). Thus, the onset and progression of serotonin degeneration parallels the course of cognitive and neuropsychiatric symptoms in the transgenic Aβ mouse model. The pattern of serotonin degeneration in mice was similar to the pattern observed in human AD patients (D'Amato et al., 1987). An association between serotonin degeneration and Aβ deposition was supported also by evidence that interventions that reduce Aβ or enhance serotonin function have a protective effect on the serotonin system or block/reduce Aβ deposition, respectively. For example, Aβ immunotherapy attenuated serotonin degeneration in the transgenic Aβ mouse model (APPswe/PS1dE9), while intrahippocampal injections of aggregated Aβ (1–42) decreased hippocampal 5-HT2A receptors; Liu et al., 2011; Christensen et al., 2008). Serotonergic agents block Aβ precursor protein processing and Aβ deposition and also improve cognitive deficits and neuropsychiatric symptoms (e.g. depression-like behaviors; Meneses, 2017). Thus, understanding the associations between serotonin and Aβ deposition may have mechanistic implications for understanding the neurobiology of cognitive deficits and neuropsychiatric symptoms.

The focus of the present study was to measure the regional distribution of serotonin degeneration (measured by 5-HTT availability) relative to Aβ deposition in the preclinical stages of AD. The decision was made to study a group with a relatively early stage of AD pathology who were "at risk" for cognitive decline, rather than an AD group that would have widespread serotonin degeneration and AD pathology, in which regional associations between 5-HTT and Aβ deposition might be difficult to measure. A group with MCI (multi-domain, amnestic MCI subtype) and a healthy, older control group underwent PET scans with well-established radiotracers to measure 5-HTT availability and Aβ deposition (Wilson et al., 2002; Klunk et al., 2004). 5-HTT is a more specific marker of serotonin degeneration than serotonin receptors, as serotonin receptors are localized also on the terminals of non-serotonergic neurons. (Azmitia & Nixon, 2008). As mentioned, 5-HTT may be more sensitive to cognitive deficits and decline than serotonin receptors. The multi-modal partial least squares method (mmPLS) was used that was developed by Chen and colleagues to examine associations between neuroimaging modalities on a voxel-wise basis (Chen et al., 2009). This study tested the hypotheses that a spatial covariance pattern of lower 5-HTT availability in cortical, limbic, subcortical (caudate and putamen) and brainstem (raphe nuclei) regions and of higher Aβ deposition in frontal, temporal and parietal cortical regions would be expressed to a greater extent in the MCI group relative to the healthy older control group and that the greater expression of the spatial covariance pattern would be correlated with greater deficits in memory and executive function.

2. Materials and methods

2.1. Participant screening and clinical characterization

Potential MCI and healthy older adult participants, age 55 years and older, underwent physical and neurological examinations, laboratory testing, toxicology screening, psychiatric and neuropsychological evaluations, as previously described (Smith et al., 2017). A Structured Clinical Interview for DSM-V (First et al., 1995), Antidepressant

Treatment History Form (Sackeim, 2001), Mini Mental State Examination (MMSE) and Clinical Dementia Rating Scale (CDR) (Folstein et al., 1975; Morris, 1993) were administered. Neuropsychiatric and mood symptoms were assessed with the Neuropsychiatric Inventory (NPI), Hamilton Depression Rating Scale (HDRS), Beck Depression Inventory (BDI) and the Apathy Evaluation scale (AES; Cummings et al., 1994; Hamilton, 1959; Beck & Steer, 1993; Marin et al., 2003). Healthy older adult participants were enrolled if they had a CDR global score of 0 (cognitively normal). MCI participants were enrolled if they had a CDR global score of 0.5 and a score of at least one standard deviation below the mean of an auditory-verbal or visual-spatial memory test and an executive function test. Auditory-verbal memory was measured with the California Verbal Learning Test (CVLT; Delis et al., 1987). Visual-spatial memory was measured with the Brief Visual Memory Test-Revised (BVMT-R; Benedict et al., 1996). Executive function was measured with the Delis-Kaplan Executive Function System (Letter and Category Fluency, Trail Making and Sorting Tests; Delis et al., 2006).

Participants in both groups were excluded from enrollment if they had: 1) a history of or current neurological or Axis I psychiatric disorder (including major depression), except for a DSM-V diagnosis of mild neurocognitive disorder in MCI participants; 2) poorly controlled medical conditions, including hypertension, diabetes and/or thyroid disease; 3) a positive toxicology screening and/or current use of psychotropic drugs (including antidepressant and antipsychotic drugs) or medications with serotonergic or central nervous system effects (including Trazadone, Tramadol, Sumatriptan, antihistamines or cold medications) within two weeks prior to enrollment and 4) contraindications for undergoing MRI scans (e.g. pacemaker, metal implants, cerebral arterial aneurysm clips). The study protocol and consent forms were approved by the Institutional Review Board and the Radiation Research Committee of the Johns Hopkins University School of Medicine. Participants received both a transcribed and verbal description of the study and written informed consent was obtained.

2.2. Genotyping

DNA from blood was extracted using the Gentra Puregene Blood Kit from Qiagen (cat# 158389; Germantown, Maryland), following the manufacturer's protocol. *APOE* genotyping was performed using polymerase chain reaction amplification of genomic DNA digestion with Hhal restriction enzyme and gel electrophoresis, as previously described (Avramopoulos et al., 1996). Genotyping of the serotonin transporter promoter polymorphism (5-HTTLPR) was performed by polymerase chain reaction amplification with primers GGCGTTGCCGCTCTGAATGC and GAGGGACTGAGCTGGACAACCAC at an annealing temperature of 60 degreesC and electrophoresis on a 2.5 % agarose—1% nusieve gel for separation of the short and long allelic variants as previously described (Peters et al., 2016).

2.3. MR imaging procedures

MRI scans of the brain were acquired, as described previously (Smith et al., 2017). A Phillips 3.0 T Achieva MRI instrument with an 8-channel head coil was used (Philips Medical Systems, Best, Netherlands). A magnetization-prepared rapid acquisition with gradient-echo (MPRAGE) pulse sequence (TE = 4, TR = 8.9, flip angle = 8 degrees, NSA = 1, 0.7 mm isotropic voxel size) was used for PET image processing.

2.4. PET acquisition and quantification

Procedures for PET scan acquisition, reconstruction and analysis have been described previously (Smith et al., 2021a; Smith et al., 2021b; Smith et al., 2021c). The scanner used was a second-generation High-Resolution Research Tomograph scanner (HRRT, Siemens Healthcare, Knoxville, TN), a cerium-doped lutetium oxyorthosilicate (Lu25i05 [Ce] or LSO) detector-based, dedicated brain PET scanner. Each subject was fitted with a thermoplastic mask modeled to their face to reduce head motion during the PET scan. Attenuation maps were generated from a six-minute transmission scan performed with a [^{137}Cs] point source prior to the emission scans.

The radiotracers ([^{11}C]-3-amino-4-(2-dimethylaminomethyl-phenylsulfanyl)-benzonitrile, [^{11}C]-DASB) and (*N*-methyl-[11C]2-(4′-methylaminophenyl)-6-hydroxybenzothiazole, [^{11}C]-PiB) were used to measure 5-HTT and Aβ deposition, respectively, and were synthesized according to published methods (Wilson et al., 2002; Klunk et al., 2004; Wilson et al., 2004). The MRI and PET scans were performed within approximately two weeks of each other. Dynamic scanning began immediately upon a 20 mCi ± 10 % and 15 mCi ± 10 % radiotracer injection, respectively for [^{11}C]-DASB and [^{11}C]-PiB, and lasted for 90 min for both radiotracers. The data were acquired in list mode. The images for both radiotracers were reconstructed using the iterative ordered subset expectation maximization (OS-EM) algorithm (with 6 iterations and 16 subsets), with correction for radioactive decay, dead time, attenuation, scatter and randoms (Rahmim et al., 2005) and rebinned into thirty frames (four 15 s, four 30 s, three 1 min, two 2 min, five 4 min, and twelve 5 min frames. The reconstructed image space consisted of 256 (left-to-right) by 256 (nasion-to-inion) by 207 (neck-to-cranium) cubic voxels, each 1.22 mm in dimension. The final spatial resolution was <2.5 mm full width at half-maximum (FWHM) in three directions (Sossi et al., 2005).

2.5. MRI processing and analysis

MPRAGE images were submitted to FreeSurfer (FS; v6.0) for automated parcellation of left and right cortical and subcortical volumes of interest (VOIs) and whole cerebellum gray matter (Fischl et al., 2002; Desikan et al., 2006). VOIs were transferred from MRI to PET space using parameters that were obtained using the co-registration module in SPM12 (SPM12; Institute of Neurology, London) running on MATLAB 7.10 (MathWorks, Natick, Massachusetts).

FS-derived gray and white matter (GM and WM, respectively) masks of individual subjects were submitted to the "Diffeomorphic Anatomical Registration Through Exponentiated Lie Algebra" (DARTEL) algorithm (Ashburner, 2007) to obtain a pair of GM and WM templates. Templates were spatially registered to Montreal Neurological Institute (MNI) space and GM and WM masks of individual subjects were spatially normalized to MNI space in the final step of DARTEL. So-obtained GM and WM masks were averaged across subjects to obtain FS-based GM and WM templates and inserted in place of SPM-supplied 6-layer templates (i.e., TPM.nii) to be FS-derived 6 layer templates. FS-derived templates were used for spatial normalization of functional images.

2.6. PET tracer kinetic modelling and image processing

Regional distribution volume ratio (DVR) values of [^{11}C]-DASB were obtained using the reference tissue graphical analysis method (RTGA; Logan et al., 1996) The cerebellar grey matter (excluding the vermis) was used as the reference region (Parsey et al., 2006). Briefly, the assumed t* (the time when the free-plasma ratio approaches time-invariant) was set to 25 min. The brain-to-blood clearance rate constant (k2R) of the cerebellum was set to 0.048 min^{-1}, which corresponded to a population mean value of k2R derived from the multilinear reference tissue method with 2 parameters (MRTM2; Ichise et al., 2003). To reduce noise-dependent underestimation of DVR seen on DVR maps from RTGA, DVR maps were generated by RTGA using dynamic PET frames that were smoothed by a 6 mm (FWHM) Gaussian kernel.

Regional DVR values of [^{11}C]-PiB were obtained by MRTM2 with the cerebellar gray matter (excluding the vermis) as reference region (Klunk et al., 2004). Briefly, the assumed t* (the time when the free-plasma ratio approaches time-invariant) was set to 25 min. The brain-to-blood clearance rate constant (k2R) of the cerebellum was set to 0.149

min^{-1}, which corresponded to a population mean value of k2R from the initial MRTM2 analyses of the dataset. To reduce the number of outliers (voxels with negative values or exceeding five times of subject's maximal regional value), dynamic PET frames were smoothed with a 6 mm Gaussian kernel prior to generating DVR maps.

Pre-processing and voxel-wise statistical analyses of parametric [^{11}C]-DASB and [^{11}C]-PiB DVR images was performed with SPM12. First, as mentioned, MRIs were spatially normalized to MNI space using FS derived, 6-layer template from DARTEL, in place of the SPM-supplied template. Second, [^{11}C]-DASB and [^{11}C]-PiB DVR images were transferred to MNI space by combining spatial normalization and PET-to-MRI co-registration parameters. Parametric images for the two tracers in MNI space were smoothed with a 5 mm (FWHM) Gaussian kernel. The combination of smoothing of dynamic PET frames with smoothing of the parametric images was equivalent to smoothing native PET images with an 8 mm (FWHM) Gaussian kernel. A binarized FS-derived GM + WM mask, after smoothing with a 10 mm (FWHM) Gaussian kernel (height threshold = 0.2) limited the search area (explicit mask).

To determine "Aβ positivity", mean cortical Aβ levels were calculated and cut-offs were applied using a method validated against post-mortem data (Villeneuve et al., 2015). A weighted mean of the following FS VOIs (right and left hemispheres) was calculated: frontal pole, rostral middle frontal, superior frontal lobe, caudal middle frontal, frontal operculum, orbital operculum, lateral orbital gyrus, medial orbital gyrus, rostral anterior cingulate, caudal anterior cingulate, superior temporal lobe, middle temporal lobe, inferior temporal lobe, isthmus/cingulate, posterior cingulate, precuneus, superior parietal lobe, inferior parietal lobe, supramarginal gyrus and lingual gyrus. A conservative Aβ cut-off was used to define "Aβ negative" (DVR $<$ 1.20) and "Aβ positive" (DVR $\geq$ 1.20) participants. The mean cortical Aβ deposition, mean cortical and hippocampal 5-HTT availability and mean gray matter cortical volumes are reported (using the same cortical VOI). The results reported herein included healthy older controls who were "Aβ negative" and individuals with MCI who were "Aβ positive" .

2.7. Multi-modal partial least squares (mmPLS)

The voxel-based, mmPLS algorithm was introduced by Chen and colleagues to combine PET scans of cerebral glucose metabolism with structural MRI scans that was recently applied to combine the same PET radiotracers as used in the present study to patients with late-life depression and healthy older controls (Chen et al., 2009, 2012; Smith et al., 2021b). These and other studies demonstrated that integrating information from different imaging modalities increased statistical power and addressed the issue of multiple comparisons associated with univariate, voxel-wise analyses. There are two types of mmPLS: informed and agnostic mmPLS. In informed mmPLS, the variable of interest (e.g. diagnostic group membership) is directly incorporated into the mmPLS process. Agnostic mmPLS, on the other hand, is performed blind to the variable of interest (diagnostic and associated clinical information). Corresponding to each of the two approaches, statistical test procedures were established to objectively assess type-I error related to the variable of interest (e.g. group differences). The algorithm generates 1) maps of the covarying pattern for each modality and 2) a single mmPLS score for each person to reflect the strength of this covarying pattern. Note the generation of the covarying pattern for each of the two modalities maximizes the covariance between the 5-HTT/Aβ paired subject scores at the group level. In this sense, the covariance metrics generated by mmPLS represent the covariance that can be standardized to form the correlation coefficient between the paired subject scores.

Agnostic mmPLS was used in this study, given that the primary interest was to assess between-group differences and to measure the relationship of the neuroimaging to the cognitive and neuropsychiatric symptom measures. In running the agnostic mmPLS for dual-modality 5-HTT and Aβ PET data, the covariance patterns were estimated blindly over all subjects (no diagnostic group or clinical information was used). The between-group difference was tested using the 5HTT – Aβ subject scores associated with each of the spatial covariance patterns. First, agnostic mmPLS was run to generate the covarying patterns between 5-HTT and Aβ. Then, between-group differences and correlations with cognitive measures and neuropsychiatric symptom ratings were evaluated using the 5HTT – Aβ subject scores, which reflect the extent to which each subject expressed the spatial covariance pattern. For the mmPLS analyses, the 'search area' or the collection of voxels over which mmPLS was performed was defined by a whole brain mask (GM and WM), excluding both the ventricular space and the voxels outside the brain. For both analyses, the voxels within the mask are defined as those with an integer value of 1 and those outside the mask as 0. More information about the mmPLS method is provided in the Supplemental Materials Section.

2.8. Statistical analysis

Between-group differences in the demographic, cognitive, neuropsychiatric, genetic and neuroimaging measures were tested using a two-sample independent sample T-tests for interval variables, and Chi-Square tests for categorical variables.

The mmPLS spatial covariance pattern (as a three-dimensional brain map) for each PET radiotracer was scaled by the brain-map wide standard deviation within the search area to form the z-score map and was displayed with a threshold of $P = 0.05$, since the correction for multiple comparisons is not relevant for the spatial covariance pattern display. The covariance metrics between the two tracers was the correlation coefficient between the paired subject scores. Since the subject scores are paired again (one for each imaging modality), group differences were initially examined using the multivariate Hotelling *T*-square test. Given the close correlation between 5-HTT availability and Aβ deposition for each subject score pair, principal component analysis (PCA) was applied to project the paired subject scores along the direction of the PCA major axis to form a single subject score to which the conventional univariate two-sample independent *t*-test could be applied. If more than one spatial covariance pattern was associated with group differences, the formation of a single pattern was attempted by taking a weighted sum of the patterns with the weights estimated by the general linear model, which included subject scores of the corresponding patterns as the predictors of group membership. Correlations were performed between the subject scores for each radiotracer and the combined subject score and selected cognitive and neuropsychiatric symptom measures. As the mmPLS method is designed to identify the maximal covariance of two spatial patterns, the 5-HTT and Aβ patterns are not entirely independent of each other and the correlations are expected to be similar. For the mmPLS spatial pattern, brain regions were labelled using the AAL and the AAL3 atlases, the latter atlas was used to identify the peak locations in the brainstem. (Tzourio-Mazoyer et al., 2002, Rolls et al., 2015; Rolls et al., 2020).

3. Results

3.1. Demographic, clinical, cognitive and neuroimaging results

Forty-five MCI and 35 healthy older adults completed clinical and cognitive evaluations, 5-HTT and Aβ PET scans. Twenty-two of the individuals with MCI were "Aβ positive" and 27 of the healthy controls were "Aβ negative" and were included in the analyses. Similar findings were obtained in the analyses performed for the total MCI and control group, as were obtained for these sub-groups (including between group comparisons for cognitive and neuropsychiatric symptom variables, the spatial covariance pattern of 5-HTT and Aβ,the 5-HTT and Aβ subject scores, and the correlation between the subject scores and cognitive and neuropsychiatric symptom variables; data not shown). Demographic characteristics, clinical and cognitive measures, PET radiotracer characteristics, and the FS-derived cortical VOI for Aβ deposition, gray

Table 1
Demographic, Clinical and Cognitive Characteristics of Participants with Mild Cognitive Impairment (MCI) and Healthy Older Controls.

	Mild Cognitive Impairment (n = 22)	Healthy Older Controls (n = 27)	T*	*P* Value
Age	70 ± 8	66 ± 7	−1.359	0.181
Sex (F/M)	7/15	13/14	1.338[a]	0.247
Education (in years)	16 ± 3	16 ± 3	−0.087	0.931
Clinical Dementia Rating-Sum of Boxes	1.45 ± 0.89	0.05 ± 0.15	−6.993	0.000
Mini-Mental Status Examination	28 ± 2	29 ± 1	3.002	0.004
CVLT Total Recall (Sum of first 5 Trials)	38 ± 11	58 ± 10	6.189	0.000
CVLT Delayed Free Recall	7 ± 4	12 ± 3	5.715	0.000
BVMT-R Total Recall (Sum of first 3 Trials)	13 ± 8	19 ± 7	2.693	0.010
BVMT-R Delayed Recall	5 ± 3	8 ± 3	3.228	0.002
DKEFS™ Letter Fluency	39 ± 12	45 ± 12	1.799	0.079
DKEFS™ Category Fluency	32 ± 11	42 ± 7	3.609	0.001
DKEFS™ Category Fluency-Switching Accuracy	10 ± 4	13 ± 2	4.414	0.000
Neuropsychiatric Inventory (NPI)	5 ± 6	1 ± 1	−3.442	0.001
Hamilton Depression Rating Scale	4 ± 4	1 ± 2	−3.474	0.001
Beck Depression Inventory	8 ± 7	3 ± 3	−3.623	0.001
Apathy Evaluation Scale	32 ± 8	25 ± 6	−3.349	0.002
APOE4 genotypes (number with an e4 versus without an e4 allele)	8/14	5/22	2.650 [a]	0.104
5-HTTLRP genotypes (number with ll/ls/ss)	6/12/4	6/14/7	1.686 [a]	0.840
[^{11}C]-DASB Injected Dose	19.06 ± 1.06	19.04 ± 2.01	−0.052	0.959
[^{11}C]-DASB Specific Activity	8974 ± 3762	9459 ± 3731	0.451	0.654
[^{11}C]-DASB Mass	0.72 ± 0.34	0.62 0.25	−1.255	0.216
[^{11}C]-PiB Injected Dose	14.84 ± 0.62	14.71 ± 0.68	−0.665	0.509
[^{11}C]-PiB Specific Activity	8516 ± 2722	8292 ± 2876	−0.251	0.803
[^{11}C]-PiB Mass	0.50 ± 0.23	0.53 ± 0.19	0.496	0.622
Global Cortical Beta-Amyloid Deposition	1.74 ± 0.41	1.12 ± 0.04	−7.763	<0.001
Global Cortical Gray Matter Volumes	296.33 ± 41.42	309,47 ± 29.58	1.294	0.202
Global Cortical Serotonin Transporter Availability	0.27 ± 0.07	0.30 ± 0.07	1.803	0.078
Hippocampal Serotonin Transporter Availability	0.35 ± 0.14	0.46 ± 0.14	2.752	0.008

*Results of Two-Sample, Independent Samples T-Test; CVLT, California Verbal Learning Test, BVMT-R, Brief Visual Memory Test-Revised; DKEFS, Delis-Kaplan Executive Function System, [a]Chi-Square Test.

matter volumes and 5-HTT availability are shown in Table 1. For 5-HTT availability, the hippocampal VOI, is also shown to provide an example of a brain region with substantial 5-HTT loss in MCI relative to controls (Smith et al., 2017). There were no significant differences between the MCI and control groups in age, sex distribution, years of education. or number of APOE4 or 5-HTTLRP alleles. As expected, the MCI group showed significantly worse cognitive function relative to the healthy control group in global measures (MMSE and the CDR sum of boxes scores), as well as domain-specific cognitive measures, including immediate and delayed free recall on the CVLT and BVMT-R, category fluency and category fluency-switching accuracy, but not in letter fluency. While two of the healthy controls had CDR sum of boxes scores of 0.5 in the judgement and problem-solving domain, both controls received a 0 in the memory domain and, therefore, the CDR global score was 0. MCI participants showed significantly greater neuropsychiatric, depressive and apathy symptoms relative to the controls, although the scores in the MCI group were in the mild range. The injected dose, specific activity and mass injected for [^{11}C]-DASB and [^{11}C]-PiB did not differ significantly between MCI and control groups. The cortical Aβ deposition was significantly greater and the hippocampal 5-HTT availability was significantly lower, while the cortical gray matter volume and cortical 5-HTT availability were non-significantly lower in the MCI group relative to the control group. Fig. 1 shows the mean PET DVR images for participants in the MCI and healthy older control groups for 5-HTT availability and Aβ deposition and an MRI tenplate.

3.2. Dual-modal, agnostic mmPLS results

Two identified patterns showed significant group differences. Integrating the paired subject scores via PCA, the group differences were: t = -6.03, df = 32.3, P ≤ 0.00001 for component 1 and t = -7.87, df = 21.97, P ≤ 0.00001 for component 2. Positive values represent greater expression of the pattern of lower 5-HTT and greater Aβ, whereas negative values represent less expression of this pattern.To further reduce the type-I error associated with the two covarying patterns, the two patterns were combined via the general linear model with the corresponding subject scores representing the independent predictors of group differences. The distribution of 5HTT – Aβ subject scores for the MCI and the control groups is shown in Fig. 2. When subject scores for 5-HTT availability and Aβ deposition were further integrated using PCA, the subject scores were found to be significantly higher in the MCI group relative to the control; group (t = -8.34, df = 21.94, P < 0.000001; Cohen's f = 1.34; 95 % Confidence Interval = 0.945, 1.73). Significant between-group differences in subject scores were observed also for both 5-HTT availability (t = -6.96, df = 21.91, P < 0.000001, Cohen's f = 1.12, 95 % Confidence Interval = 0.75, 1.48) and Aβ deposition (t = -8.95, df = 23.53, P < 0.000001 Cohen's f = 1.43; 95 % Confidence Interval = 1.02, 1.83). As stated in the Methods section, the covariance metrics, measuring the association between 5-HTT and Aβ, were the correlation coefficients between the subject score pairs (formed via the general linear model). The correlation between 5-HTT and Aβ deposition was significant (r_s = 0.81, P < 0.00001). It is important to note that in performing the correlation the signs were reversed so the correlation coefficient becomes positive. The spatial covariance pattern for the two components combined for the two groups and the peak voxel locations for between-group differences are shown in Fig. 3 and in Table 2, respectively. The spatial covariance pattern included lower 5-HTT availability in cortical regions (including sensory, motor and association cortices in frontal, temporal, parietal and occipital lobes), subcortical regions (caudate, putamen, globus pallidus, thalamus), limbic regions (insula, parahippocampal gyrus, amygdala, hippocampus) and raphe nuclei (left pontine, right dorsal and right medial) and higher Aβ deposition in mainly association cortices of the frontal, temporal, parietal and occipital lobes and sub-cortical regions (caudate).

3.3. Correlations between the multi-modal partial least squares (mmPLS) determined 5HTT – Aβ subject scores and cognitive and neuropsychiatric symptom measures

Representative global and domain-specific cognitive measures that were most sensitive to the deficits observed in MCI were chosen for correlation analysis with the 5-HTT - Aβ subject scores, as well as

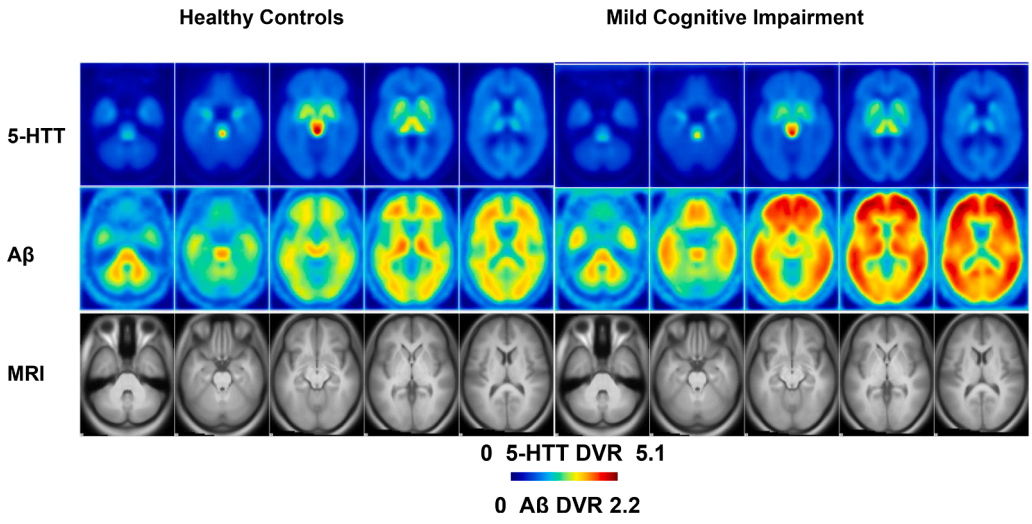

Fig. 1. Positron Emission Tomography Mean Distribution Volume Ratio (DVR) images of Serotonin Transporter availability (5-HTT; [^{11}C]-DASB) and Beta-Amyloid deposition (Aβ; [^{11}C]-PiB) and an MRI template in individuals with Mild Cognitive Impairment ("Amyloid Positive"; right panels) and healthy controls ("Amyloid Negative"; left panels).

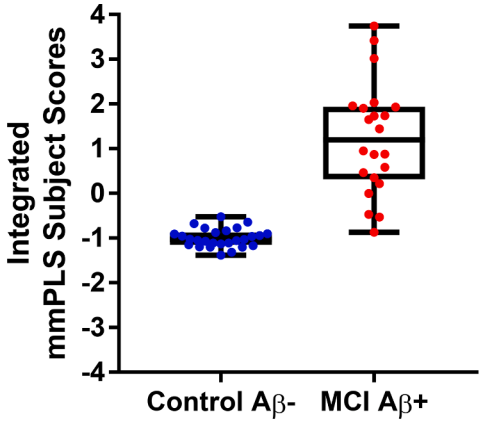

Fig. 2. The Multi-Modal Partial Least Squares (mmPLS) determined subject scores for Serotonin Transporter Availability (5-HTT) and Beta-Amyloid Deposition (Aβ) in the Mild Cognitive Impairment and Healthy Control Groups. The subject scores that are shown on the y axis represent the degree of expression of the spatial covariance pattern of 5-HTT and Aβ determined by mmPLS. The Mild Cognitive Impairment (MCI; "Amyloid Positive", Aβ +) and healthy older control ("Amyloid Negative"; Aβ-) groups are shown on the × axis. The more positive the subject score, the greater expression of the spatial covariance pattern of lower 5-HTT and higher Aβ deposition. The 5-HTT - Aβ subject scores are significantly higher in the MCI relative to the healthy control group (t = -8.34, df = 21.94, P < 0.000001).

selected measures of neuropsychiatric symptoms. The variables included MMSE, CDR sum of boxes, Long Delay Free Recall for CVLT and for BVMT-R and DKEFS Category Switching (a measure of cognitive flexibility), NPI and BDI. For the two groups combined, all of the selected global and domain-specific cognitive and neuropsychiatric symptom measures were correlated with the 5-HTT - Aβ subject scores (data not shown). Correlation results between the cognitive measures and the 5-HTT - Aβ subject scores, the 5-HTT and Aβ components in the MCI group are shown in Table 3 and between the cognitive measures and the 5-HTT - Aβ subject scores in the MCI and control groups in Fig. 4a and b. In the MCI group, significant correlations were observed between the 5-HTT - Aβ subject scores and MMSE (r_s = -0.67; $P < 0.00007$), CVLT (Long Delay Free Recall; r_s = -0.60; $P < 0.0469$), BVMT-R (Long Delay Free Recall; r_s = -0.74; $P < 0.0001$) and DKEFS Category Switching (r_s = -0.63; $P < 0.0007$), Significant correlations were not observed between the 5-HTT - Aβ subject scores and the cogntive measures in the healthy control group or between the 5-HTT - Aβ subject scores and the neuropsychiatric symptoms measures in either group alone. The correlations were similar between the cognitive measures and the 5HTT – Aβ subject scores and the 5-HTT and Aβ components.

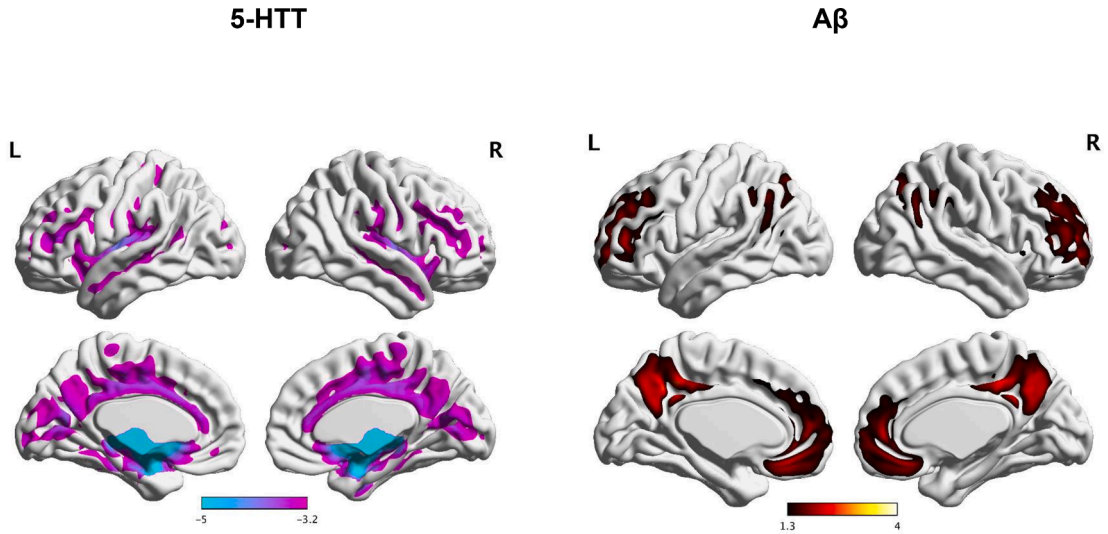

Fig. 3. The Multi-Modal Partial Least Squares (mmPLS) determined Serotonin Transporter Availability (5-HTT) and Beta-Amyloid Deposition (Aβ) Spatial Covariance Pattern that distinguished the MCI from the Healthy Control group.

4. Discussion

The goal of the present study was to determine the spatial covariance pattern of 5-HTT availability and Aβ deposition that differed between a MCI group relative to a healthy control group by applying the mmPLS method. A mmPLS determined spatial covariance pattern was expressed to a significantly greater extent in the MCI relative to the control group. The pattern was characterized by lower 5-HTT availability in cortical, striatal, thalamic, limbic (amygdala and hippocampus) regions and raphe nuclei (pontine, dorsal and medial) and greater Aβ deposition in frontal, temporal, parietal and occipital cortices. The 5-HTT availability component included limbic, striatal, thalamic and brainstem regions that have the highest concentration of 5-HTT in the brain, as well as cortical, limbic and brainstem regions that demonstrate pathology in the early stages of AD (Aβ and Tau). The Aβ component included cortical regions that accumulate Aβ in aging and MCI, based on neuropathology and molecular imaging studies.

The secondary goal of the study was to evaluate whether the expression of the 5-HTT – Aβ spatial covariance pattern identified would be correlated with cognitive deficits and neuropsychiatric symptoms. The greater expression of the pattern was significantly correlated with poorer performance in measures of global cognitive impairment, delayed auditory-verbal and visual-spatial memory and executive function in the MCI group, not in the control group. Correlations between memory and executive function measures have been observed with 5-HTT availability and with Aβ in MCI, not in controls, consistent with the present results (Smith et al., 2017, Stevens et al., 2022). The correlations between the 5-HTT and Aβ subject scores, separately, and the cognitive measures were similar to the correlations observed with the 5-HTT – Aβ subject scores. As mentioned, the mmPLS method is designed to identify the maximal covariance of two spatial patterns. Thus, the 5-HTT and Aβ components of the 5-HTT – Aβ spatial covariance pattern (and the resulting subject scores) are not entirely independent. As a result, the between-group differences for the Aβ and 5-HTT subject scores and the 5-HTT – Aβ subject scores and correlations with the cognitive measures are expected to be similar. There were significant correlations between the 5-HTT – Aβ subject scores and neuropsychiatric symptoms for the two groups combined, not separately. While the measures of neuropsychiatric symptoms (including depression and apathy) were statistically significantly higher in the MCI group than healthy controls, the scores on these measures in the MCI group would be considered to be in a mild range.

The objective of the present study was to investigate the association of serotonin degeneration with Aβ deposition, not to develop a diagnostic biomarker. Additional studies would be needed to develop the 5-HTT – Aβ spatial covariance pattern as a diagnostic biomarker, including validation in an independent subject sample, as well as pathological confirmation. The decision to focus on an MCI group in the present study was based on the considerations that an MCI group would be “at risk” for cognitive decline and would have an intermediate and heterogeneous level of serotonin degeneration and *Aβ* deposition, in contrast to more severe pathology that would be observed in AD. In fact, the results of the present study indicate that there is substantial serotonin degeneration and Aβ deposition in MCI, so that to determine whether serotonin degeneration occurs before Aβ deposition, an earlier stage of preclinical AD would need to be studied.

There are several limitations of the present study. Because of the sample size, it was not possible to compare the expression of the spatial covariance pattern as a function of APOE4 gene dose. The rate of “amyloid positivity” in the controls and ”Aβ negativity” in the MCI participants was consistent with neuroimaging and neuropathology studies (Rabinovici & Jagust, 2009; Ossenkoppele et al., 2015; Katzman et al., 1988). Limiting the analysis to only participants who are “Aβ positive” MCIs and “Aβ negative” controls yielded similar results to analyses that included all participants in the study regarding of Aβ status. These results indicate that the 5-HTT – Aβ spatial covariance pattern may be observed in the face of potentially “mixed-pathology” in MCI. Another limitation is the low level of neuropsychiatric symptoms in the MCI group that may have contributed to the lack of correlation between the 5-HTT - Aβ subject scores and neuropsychiatric symptoms. The low levels of neuropsychiatric symptoms in the enrolled MCI participants may be due to the exclusion of participants with a history of or current

Table 2
Peak Voxel Locations of Serotonin Transporter (5-HTT) Availability and Beta-Amyloid (Aβ) Deposition in Regions that Comprise the Multi-Modal Partial Least Squares (mmPLS) determined Spatial Covariance Pattern that Distinguished the Mild Cognitive Impairment (MCI) from the Healthy Control group.

a)The Component of Lower Serotonin Transporter Availability (5-HTT) in the mmPLS determined Spatial Covariance Pattern in the MCI Group Relative to the Control Group

Region Name	Left					Right				
	X	Y	Z	Z Score	P Value	X	Y	Z	Z Score	P Value
Anterior Cingulate Gyrus	0	34	16	3.73	<0.00001	0	28	−4	3.50	<0.00002
Middle Cingulate Gyrus	0	−28	40	3.84	<0.00001	4	−16	44	3.92	<0.00001
Superior Frontal Gyrus	−26	58	0	3.27	<0.00054	30	54	12	3.42	<0.00032
Middle Frontal Gyrus	−30	52	12	3.47	<0.00026	36	40	28	3.58	<0.00002
Inferior Frontal Triangularis	−44	34	16	3.60	<0.00016	46	28	24	3.59	<0.00016
Inferior Frontal Operculum	−16	10	−20	3.91	<0.00001	46	12	32	3.41	<0.00032
Supplemental Motor Area	0	−8	60	3.44	<0.00030	2	−10	52	3.76	<0.00001
Medial Orbital Frontal	−4	46	−8	3.27	<0.00054					
Rolandic Operculum	−40	−30	16	3.75	<0.00001	38	−22	20	3.41	<0.00033
Gyrus Rectus	−2	18	−20	3.34	<0.00041	20	12	−16	4.60	<0.00021
Olfactory Gyrus	4	0	−12	6.95	<0.00001	32	10	−20	4.04	<0.00001
Pre-Central Gyrus	−26	−28	60	3.44	<0.00029	26	−26	64	3.47	<0.00026
Post-Central Gyrus	−54	−8	28	3.52	<0.00022	54	−8	32	3.61	<0.00016
Paracentral Lobule	−16	−32	68	3.39	<0.00035	−2	30	68	3.49	<0.00024
Insula	−26	12	−12	4.67	<0.00001	28	14	−12	4.22	<0.00001
Heschl's Gyrus	−38	−22	8	4.00	<0.00001	44	−20	4	3.57	<0.00018
Superior Temporal Pole	−38	4	−20	4.02	<0.00001	38	6	−24	3.78	<0.0001
Superior Temporal Gyrus	−38	−8	−12	4.44	<0.00001	44	−18	−4	3.65	<0.00013
Middle Temporal Gyrus	−54	−34	0	3.46	<0.00027	48	−16	−12	3.33	<0.00044
Inferior Temporal Gyrus	−38	−12	−20	3.65	<0.00013					
Amygdala	−22	−4	−12	7.60	<0.00001	20	0	−12	7.63	<0.00001
Hippocampus	−4	−16	−16	6.73	<0.00001	12	−18	−12	6.49	<0.00001
Parahippocampal Gyrus	−28	−6	−32	4.64	<0.00001	12	−20	−16	5.10	<0.00001
Precuneus	0	−52	20	3.61	<0.00015	4	−44	40	3.55	<0.00019
Fusiform Gyrus	−30	−12	−36	3.98	<0.00001	30	−2	−40	3.81	<0.00001
Posterior Cingulate Gyrus	0	−48	28	3.66	<0.00001					
Supramarginal Gyrus	−56	−28	20	3.46	<0.00027	58	−22	28	3.39	<0.00037
Cuneus	−8	−68	24	3.85	<0.00001	14	−62	20	3.46	<0.00027
Calcarine Gyrus	−10	−66	20	3.91	<0.00001	8	−76	8	3.65	<0.00013
Superior Occipital Gyrus	−12	−96	4	3.42	<0.00031	28	−84	20	3.25	<0.00058
Middle Occipital Gyrus	−12	−96	0	3.46	<0.00027	28	−88	12	3.34	<0.00041
Inferior Occipital Gyrus	−12	−96	−8	3.33	<0.00043					
Lingual Gyrus	−6	−68	8	3.77	<0.00001	16	−58	4	3.50	<0.0001
Caudate	−10	8	−12	5.76	<0.00001	8	4	−8	8.11	<0.00001
Putamen	−22	6	−4	6.83	<0.00001	26	4	0	5.86	<0.00001
Globus Pallidus	−16	0	−8	7.85	<0.00001	24	0	−8	7.10	<0.00001
Thalamus	0	−26	−8	10.70	<0.00001	2	−14	−4	9.24	<0.00001
Pontine Raphe Nucleus	−2	−30	−24	7.33	<0.00001					
Dorsal Raphe Nucleus						0	−28	−12	11.30	<0.00001
Medial Raphe Nucleus						0	−30	−20	9.36	<0.00001

b)The Component of Greater Beta-Amyloid Deposition in the mmPLS determined Spatial Covariance Pattern in the MCI Group Relative to the Control Group

Region Name	Left					Right				
	X	Y	Z	Z Score	P Value	X	Y	Z	Z Score	P Value
Anterior Cingulate Gyrus	−4	48	4	2.15	0.0157	8	46	12	2.01	0.0221
Middle Cingulate Gyrus						8	−40	40	2.32	0.0102
Superior Frontal Gyrus	−26	56	0	2.12	0.0171	30	54	8	2.16	0.0154
Superior Medial Frontal Gyrus	−6	50	8	2.08	0.0188	12	66	8	1.86	0.0312
Middle Frontal Gyrus	−30	54	4	2.16	0.0153	30	56	4	2.12	0.0172
Superior Orbital Frontal Gyrus	−24	58	−4	2.03	0.0209	26	58	−4	1.94	0.0260
Medial Orbital Frontal Gyrus	−2	38	−12	2.18	0.0145					
Inferior Frontal Triangularis	−42	42	8	1.89	0.0296	46	38	16	1.76	0.0390
Gyrus Rectus	−50	−58	20	1.76	0.0139					
Middle Temporal Gyrus	−50	−58	20	1.76	0.0395					
Precuneus	−6	−48	40	2.95	0.0014	6	−60	40	2.31	0.0010
Posterior Cingulate	−2	−54	32	2.61	0.0045					
Inferior Parietal Lobule	−48	−56	40	1.79	0.0366	48	−52	44	1.81	0.0348
Angular Gyrus	−50	−58	24	1.79	0.0364	50	−60	36	1.81	0.0355
Superior Occipital Gyrus						24	−66	44	1.89	0.0297
Caudate	−12	14	−8	1.83	0.0338					

psychiatric diagnosis or use a of antidepressants and other psychotropic and serotonergic medications, all of which would have affected 5-HTT availability.

The 5-HTT - Aβ spatial covariance pattern observed in the present study in MCI relative to healthy controls overlaps with, but was more extensive than the mmPLS derived 5-HTT – Aβ spatial covariance pattern that was expressed in a group of late-life depressed patients to a greater extent relative to a group of healthy older adults. In the late-life depression study, the 5-HTT – Aβ subject scores were correlated with severity of depressive symptoms, not with the cognitive measures (e.g. memory and executive function), as the majority of patients were cognitively normal. The late-life depression group relative to the control group showed more localized subcortical decreases in 5-HTT availability, as well as more localized cortical Aβ deposition than the differences

Table 3
Correlations between Multi-Modal Partial Least Squares (mmPLS) Determined Subject Scores and Cognitive Measures for Participants with Mild Cognitive Impairment (MCI).

	Integrated		Beta-Amyloid		Serotonin Transporter Availability	
Cognitive Measures	R_s	P-value	R_s	*P-value*	R_s	*P-value*
Mini-Mental Status Examination (MMSE)	−0.67	<0.00007	−0.64	<0.0012	−0.63	<0.0002
CDR (Sum of Boxes)	0.38	< 0.0789	0.42	<0.0053	0.27	<0.0222
CVLT (Long Delay Free Recall)	−0.60	< 0.0469	−0.38	<0.0795	−0.38	<0.0790
BVMT-R (Long Delay Free Recall)	−0.74	< 0.0001	−0.69	< 0.0004	−0.71	<0.0002
DKEFS Fluency Total Switching	−0.-627	<0.0007	−0.68	< 0.0001	−0.64	<0.0014

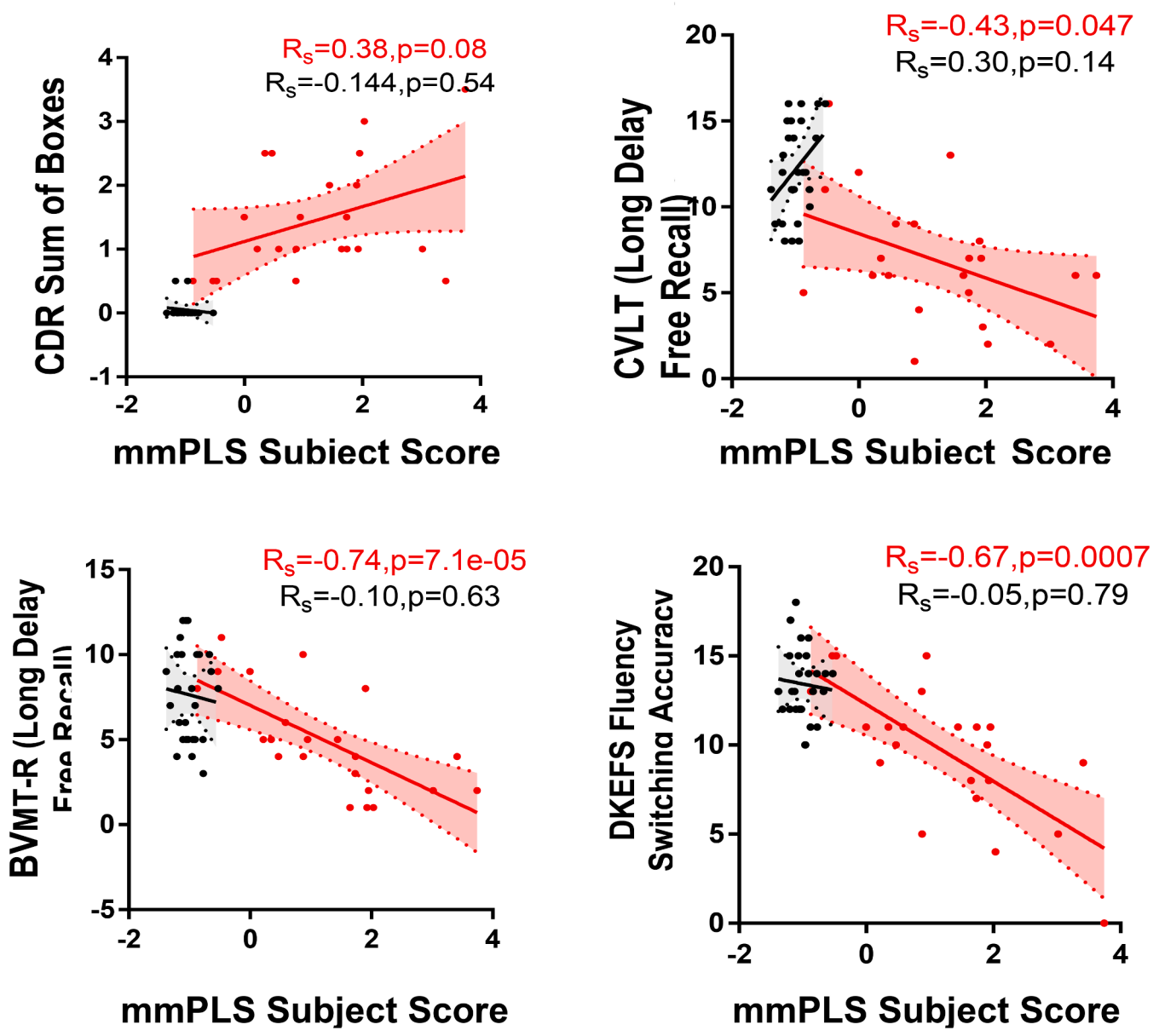

Fig. 4. Correlations between the Multi-Modal Partial Least Squares (mmPLS) Determined 5HTT – Aβ Subject Scores and Cognitive Measures for "Amyloid Positive" Mild Cognitive Impairment Participants and "Amyloid Negative" Healthy Controls.

observed between the MCI group relative to the control group in the present study. The 5-HTT - Aβ spatial covariance pattern in the MCI and control group also involved cortical and limbic 5-HTT. The evaluation of the 5-HTT - Aβ spatial covariance pattern in a group with late-life depression and cognitive deficits would be informative to determine whether the pattern showed greater association with cognition than depressive symptoms and whether the pattern has prognostic values with respect to cognitive decline.

While the present results do not imply causality and may represent two *co*-occurring pathologies, there are several potential neurobiological mechanisms to explain the association between serotonin degeneration and Aβ deposition. Neuropathology of the isodendritic core of the

brainstem (including the raphe nuclei) is a common feature of neurodegenerative and psychiatric disorders due to susceptibility to damage by reactive oxygen species (Cadet, 1988). In MCI, 5-HTT loss may lead initially to increased serotonin levels and increased serotonin metabolism via monoamine oxidase that would result in production of hydrogen peroxide and then, production of toxic hydroxyl radicals, followed by increased oxidative stress. Subsequently, serotonin levels would be decreased, secondary to serotonin neuron loss. Oxidative stress markers are increased in AD brains and are co-localized with both Aβ and Tau and may be associated with serotonin degeneration in cell bodies or in the cortical terminal projections (Green et al., 2004; M. A. Smith et al., 1994; Smith et al., 1998). Another potential mechanisms of serotonin toxicity is increased tryptophan 2,3 dioxygenase (TDO), the key regulatory enzyme in the kynurenine pathway that is highly expressed in the hippocampus of triple transgenic AD mouse models and AD patients and may be associated with Aβ and Tau formation (Wu et al., 2013). Hypotheses regarding the role of TDO or ROS could be tested *in vivo* in the future with PET radiotracers for these targets that are in development (Qiao et al., 2020; Wilson et al., 2017).

Understanding the role of serotonin degeneration in the preclinical course of AD and the relationship to Aβ deposition may have therapeutic implications as pre-clinical studies have shown that serotonergic agents may have neurobiological effects potentially relevant to prevention and symptomatic treatment of both cognitive deficits and neuropsychiatric symptoms, including inhibiting AD pathology, promoting synaptic plasticity and modulating the function of other neurotransmitters implicated in MCI and AD. 5-HT4 partial agonists, 5-HT6 antagonists and selective serotonin reuptake inhibitors (SSRI's) improve learning and memory and block AD pathology (Cho & Hu, 2007; Geldenhuys & Van Der Schyf, 2009; King et al., 2008; Lucas et al., 2010; Nelson et al., 2007; Robert and Lezoualc'h, 2008). SSRI's alter Aβ clearance in transgenic Aβ mouse models and in humans (Cirrito et al., 2020; Sheline et al., 2020). Consistent with the widespread neuroanatomic distribution of 5-HTT and serotonin receptors, serotonin modulates other neurotransmitters implicated in cognitive deficits and neuropsychiatric symptoms, including glutamate, norepinephrine, dopamine and acetylcholine (Golembiowska & Dziubina, 2000; Hilgert et al., 2000; Invernizzi et al., 1997; Lucas et al., 2000; Mateo et al., 2000). Serotonin signaling pathways activate cyclic AMP response element binding protein (CREB) and up-regulate brain derived neurotrophic factor expression (BDNF). These pathways may be impaired in the preclincial stages of AD and may lead to synaptic dysfunction and neuronal death (Mattson et al., 2004).

Several future directions follow from the present results. The 5-HTT – Aβ spatial covariance pattern should be studied longitudinally to determine whether changes in the pattern are associated with cognitive decline and emergence of neuropsychiatric symptoms in MCI and healthy controls. As mentioned, given the widespread serotonin degeneration and Aβ deposition observed in MCI, studying individuals earlier in the preclinical stages of AD may inform whether serotonin degeneration can be detected before Aβ deposition. Studying such associations in cognitively normal APOE4 carriers, who have decreased cerebral glucose metabolism in regions also affected in AD, may be informative (Reiman et al., 1996). Studying associations between 5-HTT and Aβ may be relevant to other neurodegenerative diseases associated with mood symptoms and cognitive decline. For example, in patients with Parkinson's Disease, lower cortical, striatal and midbrain 5-HTT availability was associated with higher cortical Aβ deposition (Kotagal et al., 2012). Studies are in progress to evaluate associations between Tau and 5-HTT, as Tau has been detected in the dorsal raphe nucleus prior to the transentorhinal cortex, the earliest site of cortical Tau deposition, and associations between Tau and serotonin degeneration have been shown in transgenic Aβ mouse models (Grinberg et al., 2009; Rüb et al., 2000; Simic et al., 2009; Ramos-Rodriguez et al., 2013).

5. Conclusions

A spatial covariance pattern was identified that distinguished a MCI from a healthy control group and that was characterized by lower 5-HTT availability in cortical, striatal, thalamic, limbic and raphe nuclei (pontine, dorsal andmedial) and greater cortical Aβ deposition. The pattern was expressed to a significantly greater extent in the MCI relative to the control group and was correlated with impairment in memory and executive function in the MCI group. The results support the further application of mmPLS to understand the neurochemical changes associated with Aβ deposition. An understanding of the role of serotonin degeneration in relation to AD pathology in the preclinical stages of AD is critical, given the potential application of serotonergic agents to target multiple neurobiological mechanisms relevant to prevention and symptomatic treatment of both cognitive deficits and neuropsychiatric symptoms.

CRediT authorship contribution statement

Gwenn S. Smith: Conceptualization, Methodology, Validation, Formal analysis, Investigation, Data curation, Writing – original draft, Writing – review & editing, Project administration, Funding acquisition. **Hillary Protas:** Methodology, Validation, Formal analysis, Visualization, Writing – original draft, Writing – review & editing. **Hiroto Kuwabara:** Methodology, Validation, Formal analysis, Visualization, Writing – original draft, Writing – review & editing. **Alena Savonenko:** Writing – original draft, Writing – review & editing. **Najlla Nassery:** Investigation, Writing – original draft, Writing – review & editing. **Neda F. Gould:** Investigation, Writing – original draft, Writing – review & editing. **Michael Kraut:** Investigation, Writing – original draft, Writing – review & editing. **Dimitri Avramopoulos:** Investigation, Writing – original draft, Writing – review & editing. **Daniel Holt:** Investigation. **Robert F. Dannals:** Investigation. **Ayon Nandi:** Methodology, Validation, Formal analysis, Investigation, Data curation. **Yi Su:** Writing – original draft, Writing – review & editing. **Eric M. Reiman:** Writing – original draft, Writing – review & editing. **Kewei Chen:** Methodology, Validation, Formal analysis, Visualization, Writing – original draft, Writing – review & editing.

Declaration of Competing Interest

The authors declare that they have no known competing financial interests or personal relationships that could have appeared to influence the work reported in this paper.

Data availability

Data will be made available on request.

Acknowledgements

The authors gratefully acknowledge Karen Edmonds, Bineyam Gebrewold, Michael Hans, Corina Voicu and David J. Clough for their invaluable contribution to the acquisition of PET data and to Terri Brawner, Ivana Kusevic and Kathy Kahl for their invaluable contribution to the acquisition of MRI data.

Funding

This study was supported by: National Institute of Health: MH064823 (GSS), MH086881 (GSS), AG038893 (GSS), AG041633 (GSS), AG059390 (GSS), UL1 TR 001079 (DEF), P30 AG072980 (Arizona Alzheimer's Disease Research Center [EMR]) and the State of Arizona.

References

Ashburner, J., 2007. A fast diffeomorphic image registration algorithm. NeuroImage 38 (1), 95–113.

Avramopoulos, D., Grigoriadou, M., Petersen, M.B., Mikkelsen, M., Petersen, M.B., Vassilopoulos, D., 1996. Apolipoprotein E allele distribution in parents of Down's syndrome children. Lancet 347 (9005), 862–865.

Azmitia, E.C., Nixon, R., 2008. Dystrophic serotonergic axons in neurodegenerative diseases. Brain Research 1217, 185–194.

Beck, A.T., Steer, R.A., 1993. Manual for the Beck Depression Inventory. Psychological Corporation, San Antonio, TX.

Benedict, R.H.B., Schretlen, D., Groninger, L., Dobraski, M., Shpritz, B., 1996. Revision of the brief visuospatial memory test: Studies of normal performance, reliability, and validity. Psychological Assessment 8 (2), 145–153.

Blin, J., Baron, J.C., Dubois, B., Crouzel, C., Fiorelli, M., Attar-Lévy, D., Pillon, B., Fournier, D., Vidailhet, M., Agid, Y., 1993. Loss of brain 5-HT2receptors in alzheimer's disease: In vivo assessment with positron emission tomography and (18) setoperone. Brain 116 (3), 497–510.

Bowen, D.M., Allen, S.J., Benton, J.S., Goodhardt, M.J., Haan, E.A., Palmer, A.M., Sims, N.R., Smith, C.C.T., Spillane, J.A., Esiri, M.M., Neary, D., Snowdon, J.S., Wilcock, G.K., Davison, A.N., 1983. Biochemical Assessment of Serotonergic and Cholinergic Dysfunction and Cerebral Atrophy in Alzheimer's Disease. Journal of Neurochemistry 41 (1), 266–272.

Brier, M.R., Gordon, B., Friedrichsen, K., McCarthy, J., Stern, A., Christensen, J., Owen, C., Aldea, P., Su, Y., Hassenstab, J., Cairns, N.J., Holtzman, D.M., Fagan, A. M., Morris, J.C., Benzinger, T.L.S., Ances, B.M., 2016. Tau and Ab imaging, CSF measures, and cognition in Alzheimer's disease. Science Translational Medicine. https://doi.org/10.1126/scitranslmed.aaf2362.

Cadet, J.L., 1988. A unifying theory of movement and madness: Involvement of free radicals in disorders of the isodendritic core of the brainstem. Medical Hypotheses 27 (1), 59–63.

Chen, K., Reiman, E.M., Huan, Z., Caselli, R.J., Bandy, D., Ayutyanont, N., Alexander, G. E., 2009. Linking functional and structural brain images with multivariate network analyses: A novel application of the partial least square method. NeuroImage 47 (2), 602–610.

Chen, K., Ayutyanont, N., Langbaum, J.B.S., Fleisher, A.S., Reschke, C., Lee, W., Liu, X., Alexander, G.E., Bandy, D., Caselli, R.J., Reiman, E.M., 2012. Correlations between FDG PET glucose uptake-MRI gray matter volume scores and apolipoprotein E ε4 gene dose in cognitively normal adults: A cross-validation study using voxel-based multi-modal partial least squares. NeuroImage 60 (4), 2316–2322.

Cho, S., Hu, Y., 2007. Activation of 5-HT4 receptors inhibits secretion of β-amyloid peptides and increases neuronal survival. Experimental Neurology 203 (1), 274–278.

Christensen, R., Marcussen, A.B., Wörtwein, G., Knudsen, G.M., Aznar, S., 2008. Aβ (1–42) injection causes memory impairment, lowered cortical and serum BDNF levels, and decreased hippocampal 5-HT2A levels. Experimental Neurology 210 (1), 164–171.

Cirrito, J.R., Wallace, C.E., Yan, P., Davis, T.A., Gardiner, W.D., Doherty, B.M., King, D., Yuede, C.M., Lee, J.-M., Sheline, Y.I., 2020. Effect of escitalopram on Aβ levels and plaque load in an Alzheimer mouse model. In *Neurology* 95 (19), e2666 e2674.

Cummings, J.L., Mega, M., Gray, K., Rosenberg-Thompson, S., Carusi, D.A., Gornbein, J., 1994. The neuropsychiatric inventory: Comprehensive assessment of psychopathology in dementia. Neurology 44 (12), 2308.

Curcio, C.A., Kemper, THOMAS, 1984. Nucleus raphe dorsalis in dementia of the alzheimer type: Neurofibrillary changes and neuronal packing density. Journal of Neuropathology and Experimental Neurology 43 (4), 359–368.

D'Amato, R.J., Zweig, R.M., Whitehouse, P.J., Wenk, G.L., Singer, H.S., Mayeux, R., Price, D.L., Snyder, S.H., 1987. Aminergic systems in Alzheimer's disease and Parkinson's disease. Annals of Neurology 22 (2), 229–236.

Delis, D.C., Kaplan, E., Kramer, J.H., 2006. Delis Kaplan Executive Function System (D-KEFS) Test Review. Applied. Neuropsychology.

Delis, D., Kramer, J., Kaplan, E., Ober, B., 1987. California Verbal Learning Test (CVLT) Manual. The Psychological Corporation. https://doi.org/10.1207/s15328023top2503_18.

Desikan, R.S., Ségonne, F., Fischl, B., Quinn, B.T., Dickerson, B.C., Blacker, D., Buckner, R.L., Dale, A.M., Maguire, R.P., Hyman, B.T., Albert, M.S., Killiany, R.J., 2006. An automated labeling system for subdividing the human cerebral cortex on MRI scans into gyral based regions of interest. NeuroImage 31 (3), 968–980.

Engler, H., Forsberg, A., Almkvist, O., Blomquist, G., Larsson, E., Savitcheva, I., Wall, A., Ringheim, A., Langstrom, B., Nordberg, A., 2006. Two-year follow-up of amyloid deposition in patients with Alzheimer's disease. Brain 129 (11), 2856–2866.

First, M., Spitzer, R., Gibbon, M., Williams, J., Davies, Borus, J., Howes, M. J., Kane, J., Pope, H. G., & Rounsaville, B. (1995). The Structured Clinical Interview for DSM-IV Axis I Disorders-Patient Edition. In *Biometrics Research Department*. https://doi.org/10.1521/pedi.1995.9.2.92.

Fischl, B., Salat, D.H., Busa, E., Albert, M., Dieterich, M., Haselgrove, C., van der Kouwe, A., Killiany, R., Kennedy, D., Klaveness, S., Montillo, A., Makris, N., Rosen, B., Dale, A.M., 2002. Whole brain segmentation: Automated labeling of neuroanatomical structures in the human brain. Neuron 33 (3), 341–355.

Folstein, M.F., Folstein, S.E., McHugh, P.R., 1975. "Mini-mental state". A practical method for grading the cognitive state of patients for the clinician. Journal of Psychiatric Research. 12 (3), 189–198.

Garcia-Alloza, M., Hirst, W.D., Chen, C.P.L.H., Lasheras, B., Francis, P.T., Ramírez, M.J., 2004. Differential Involvement of 5-HT1B/1D and 5-HT6 Receptors in Cognitive and Non-cognitive Symptoms in Alzheimer's Disease. Neuropsychopharmacology 29 (2), 410–416. https://doi.org/10.1038/sj.npp.1300330.

Geldenhuys, W.J., Van der Schyf, C.J., 2009. The serotonin 5-HT6 receptor: A viable drug target for treating cognitive deficits in Alzheimer's disease. In *Expert Review of Neurotherapeutics* 9 (7), 1073–1085.

Golembiowska, K., Dziubina, A., 2000. Effect of acute and chronic administration of citalopram on glutamate and aspartate release in the rat prefrontal cortex. Polish Journal of. Pharmacology.

Green, P.S., Mendez, A.J., Jacob, J.S., Crowley, J.R., Growdon, W., Hyman, B.T., Heinecke, J.W., 2004. Neuronal expression of myeloperoxidase is increased in Alzheimer's disease. Journal of Neurochemistry 90 (3), 724–733.

Grinberg, L. T., Rüb, U., Ferretti, R. E. L., Nitrini, R., Farfel, J. M., Polichiso, L., Gierga, K., Jacob-Filho, W., & Heinsen, H. (2009). The dorsal raphe nucleus shows phospho-tau neurofibrillary changes before the transentorhinal region in Alzheimer's disease. A precocious onset? *Neuropathology and Applied Neurobiology*. https://doi.org/10.1111/j.1365-2990.2008.00997.x.

Hamilton. (1959). Hamilton M. A rating scale for depression. J Neurol Neurosurg Psychiatry 1960; 23:56–62. In *ECDEU Assessment Manual for Psychopharmacology*.

Hasselbalch, S.G., Madsen, K., Svarer, C., Pinborg, L.H., Holm, S., Paulson, O.B., Waldemar, G., Knudsen, G.M., 2008. Reduced 5-HT2A receptor binding in patients with mild cognitive impairment. Neurobiology of Aging 29 (12), 1830–1838.

Hilgert, M., Buchholzer, M., Jeltsch, H., Kelche, C., Cassel, J.-C., Klein, J., 2000. Serotonergic modulation of hippocampal acetylcholine release after long-term neuronal grafting. NeuroReport 11 (14), 3063–3065.

Hirao, K., Pontone, G.M., Smith, G.S., 2015. Molecular imaging of neuropsychiatric symptoms in Alzheimer's and Parkinson's disease. Neuroscience and Biobehavioral Reviews 49, 157–170.

Holmes, C., Boche, D., Wilkinson, D., Yadegarfar, G., Hopkins, V., Bayer, A., Jones, R.W., Bullock, R., Love, S., Neal, J.W., Zotova, E., Nicoll, J.AR., 2008. Long-term effects of Aβ42 immunisation in Alzheimer's disease: follow-up of a randomised, placebo-controlled phase I trial. The Lancet 372 (9634), 216–223.

Ichise, M., Liow, J.-S., Lu, J.-Q., Takano, A., Model, K., Toyama, H., Suhara, T., Suzuki, K., Innis, R.B., Carson, R.E., 2003. Linearized reference tissue parametric imaging methods: Application to [11C]DASB positron emission tomography studies of the serotonin transporter in human brain. Journal of Cerebral Blood Flow and Metabolism 23 (9), 1096–1112.

Insel, P.S., Ossenkoppele, R., Gessert, D., Jagust, W., Landau, S., Hansson, O., Weiner, M. W., Mattsson, N., 2017. Time to amyloid positivity and preclinical changes in brain metabolism, atrophy, and cognition: Evidence for emerging amyloid pathology in alzheimer's disease. Frontiers in Neuroscience. https://doi.org/10.3389/fnins.2017.00281.

Invernizzi, R., Velasco, C., Bramante, M., Longo, A., Samanin, R., 1997. Effect of 5-HT (1A) receptor antagonists on citalopram-induced increase in extracellular serotonin in the frontal cortex, striatum and dorsal hippocampus. Neuropharmacology 36 (4-5), 467–473.

Jack, C.R., Lowe, V.J., Weigand, S.D., Wiste, H.J., Senjem, M.L., Knopman, D.S., Shiung, M.M., Gunter, J.L., Boeve, B.F., Kemp, B.J., Weiner, M., Petersen, R.C., 2009. Serial PIB and MRI in normal, mild cognitive impairment and Alzheimers disease: Implications for sequence of pathological events in Alzheimers disease. Brain 132 (5), 1355–1365.

Jagust, W., 2016. Is amyloid-β harmful to the brain? Brain 139 (1), 23–30.

Katzman, R., Terry, R., DeTeresa, R., Brown, T., Davies, P., Fuld, P., Renbing, X., Peck, A., 1988. Clinical, pathological, and neurochemical changes in dementia: A subgroup with preserved mental status and numerous neocortical plaques. Annals of Neurology 23 (2), 138–144.

Kepe, V., Barrio, J.R., Huang, S.-C., Ercoli, L., Siddarth, P., Shoghi-Jadid, K., Cole, G.M., Satyamurthy, N., Cummings, J.L., Small, G.W., Phelps, M.E., 2006. Serotonin 1A receptors in the living brain of Alzheimer's disease patients. Proc. Natl. Acad. Sci. U. S.A. 103 (3), 702–707.

King, M., Marsden, C., Fone, K., 2008. A role for the 5-HT1A, 5-HT4 and 5-HT6 receptors in learning and memory. In *Trends in Pharmacological Sciences* 29 (9), 482–492.

Klunk, W.E., Engler, H., Nordberg, A., Wang, Y., Blomqvist, G., Holt, D.P., Bergström, M., Savitcheva, I., Huang, G.-F., Estrada, S., Ausén, B., Debnath, M.L., Barletta, J., Price, J.C., Sandell, J., Lopresti, B.J., Wall, A., Koivisto, P., Antoni, G., Mathis, C.A., Långström, B., 2004. Imaging Brain Amyloid in Alzheimer's Disease with Pittsburgh Compound-B. Annals of Neurology 55 (3), 306–319.

Kotagal, V., Bohnen, N.I., Müller, M.L.T.M., Koeppe, R.A., Frey, K.A., Albin, R.L., 2012. Cerebral amyloid deposition and serotoninergic innervation in Parkinson disease. Archives of Neurology 69 (12), 1628.

Liu, Y., Yoo, M.-J., Savonenko, A., Stirling, W., Price, D.L., Borchelt, D.R., Mamounas, L., Lyons, W.E., Blue, M.E., Lee, M.K., 2008. Amyloid pathology is associated with progressive monoaminergic neurodegeneration in a transgenic mouse model of Alzheimer's disease. Journal of Neuroscience 28 (51), 13805–13814.

Liu, Y., Lee, M.K., James, M.M., Price, D.L., Borchelt, D.R., Troncoso, J.C., Oh, E.S., 2011. Passive (Amyloid-β Immunotherapy attenuates monoaminergic axonal degeneration in the AβPPswe/PS1dE9 mice. Journal of Alzheimer's Disease 23 (2), 271–279. https://doi.org/10.3233/JAD-2010-101602.

Logan, J., Fowler, J.S., Volkow, N.D., Wang, G.-J., Ding, Y.-S., Alexoff, D.L., 1996. Distribution volume ratios without blood sampling from graphical analysis of PET data. Journal of Cerebral Blood Flow and Metabolism 16 (5), 834–840.

Lucas, G., De Deurwaerdère, P., Porras, G., Spampinato, U., 2000. Endogenous serotonin enhances the release of dopamine in the striatum only when nigro-striatal dopaminergic transmission is activated. Neuropharmacology 39 (11), 1984–1995.

Lucas, G., Du, J., Romeas, T., Mnie-Filali, O., Haddjeri, N., Piñeyro, G., Debonnel, G., Okazawa, H., 2010. Selective serotonin reuptake inhibitors potentiate the rapid antidepressant-like effects of serotonin4 receptor agonists in the rat. PLoS ONE 5 (2), e9253.

Lucki, I., 1998. The spectrum of behaviors influenced by serotonin. Biological Psychiatry 44 (3), 151–162.

Lyness, S.A., Zarow, C., Chui, H.C., 2003. Neuron loss in key cholinergic and aminergic nuclei in Alzheimer disease: A meta-analysis. In *Neurobiology of Aging*. https://doi.org/10.1016/S0197-4580(02)00057-X.

Madsen, K., Neumann, W.-J., Holst, K., Marner, L., Haahr, M.T., Lehel, S., Knudsen, G.M., Hasselbalch, S.G., 2011. Cerebral serotonin 4 receptors and amyloid-β in early Alzheimer's disease. Journal of Alzheimer's Disease 26 (3), 457–466.

Mann, D.M., Yates, P.O., 1983. Serotonin nerve cells in Alzheimer's disease. In *Journal of neurology, neurosurgery, and psychiatry*. 46 (1), 96.

Marin, R.S., Butters, M.A., Mulsant, B.H., Pollock, B.G., Reynolds, C.F., 2003. Apathy and Executive Function in Depressed Elderly. Journal of Geriatric Psychiatry and Neurology 16 (2), 112–116.

Marner, L., Knudsen, G.M., Madsen, K., Holm, S., Baaré, W., Hasselbalch, S.G., 2011. The reduction of Baseline serotonin 2A receptors in mild cognitive impairment is stable at two-year follow-up. Journal of Alzheimer's Disease 23 (3), 453–459.

Mateo, Y., Ruiz-Ortega, J.A., Pineda, J., Ugedo, L., Meana, J.J., 2000. Inhibition of 5-hydroxytryptamine reuptake by the antidepressant citalopram in the locus coeruleus modulates the rat brain noradrenergic transmission in vivo. Neuropharmacology 39 (11), 2036–2043.

Mattson, M.P., Maudsley, S., Martin, B., 2004. BDNF and 5-HT: A dynamic duo in age-related neuronal plasticity and neurodegenerative disorders. Trends in Neurosciences 27 (10), 589–594.

Meneses, A., 2017. Frameworking memory and serotonergic markers. Reviews in the Neurosciences 28 (5), 455–497. https://doi.org/10.1515/revneuro-2016-0079.

Metaxas, A., Anzalone, M., Vaitheeswaran, R., Petersen, S., Landau, A.M., Finsen, B., 2019. Neuroinflammation and amyloid-beta 40 are associated with reduced serotonin transporter (SERT) activity in a transgenic model of familial Alzheimer's disease. Alzheimer's Research and Therapy 11 (1). https://doi.org/10.1186/s13195-019-0491-2.

Molliver, M.E., 1987. Serotonergic neuronal systems: What their anatomic organization tells us about function. Journal of Clinical Psychopharmacology 7 (Supplement 6), 24S.

Mormino, E.C., Kluth, J.T., Madison, C.M., Rabinovici, G.D., Baker, S.L., Miller, B.L., Koeppe, R.A., Mathis, C.A., Weiner, M.W., Jagust, W.J., 2009. Episodic memory loss is related to hippocampal-mediated β-amyloid deposition in elderly subjects. Brain. https://doi.org/10.1093/brain/awn320.

Morris, J.C., 1993. The Clinical Dementia Rating (CDR): current version and scoring rules. Neurol 43 (11), 2412–2414.

Nelson, R.L., Guo, Z., Halagappa, V.M., Pearson, M., Gray, A.J., Matsuoka, Y., Brown, M., Martin, B., Iyun, T., Maudsley, S., Clark, R.F., Mattson, M.P., 2007. Prophylactic treatment with paroxetine ameliorates behavioral deficits and retards the development of amyloid and tau pathologies in 3xTgAD mice. Experimental Neurology. https://doi.org/10.1016/j.expneurol.2007.01.037.

Ossenkoppele, R., Jansen, W.J., Rabinovici, G.D., Knol, D.L., van der Flier, W.M., van Berckel, B.N.M., Scheltens, P., Visser, P.J., Verfaillie, S.C.J., Zwan, M.D., Adriaanse, S.M., Lammertsma, A.A., Barkhof, F., Jagust, W.J., Miller, B.L., Rosen, H. J., Landau, S.M., Villemagne, V.L., Rowe, C.C., Lee, D.Y., Na, D.L., Seo, S.W., Sarazin, M., Roe, C.M., Sabri, O., Barthel, H., Koglin, N., Hodges, J., Leyton, C.E., Vandenberghe, R., van Laere, K., Drzezga, A., Forster, S., Grimmer, T., Sánchez-Juan, P., Carril, J.M., Mok, V., Camus, V., Klunk, W.E., Cohen, A.D., Meyer, P.T., Hellwig, S., Newberg, A., Frederiksen, K.S., Fleisher, A.S., Mintun, M.A., Wolk, D.A., Nordberg, A., Rinne, J.O., Chételat, G., Lleo, A., Blesa, R., Fortea, J., Madsen, K., Rodrigue, K.M., Brooks, D.J., 2015. Prevalence of amyloid PET positivity in dementia syndromes: a meta-analysis. JAMA 313 (19), 1939.

Ouchi Y, Yoshikawa E, Futatsubashi M, Yagi S, Ueki T, Nakamura K. Altered brain **serotonin transporter** and associated glucose metabolism in **Alzheimer disease**. J Nucl Med. 2009 Aug;50(8):1260-6. doi: 10.2967/jnumed.109.063008. Epub 2009 Jul 17.PMID: 19617327.

Parsey, R.V., Kent, J.M., Oquendo, M.A., Richards, M.C., Pratap, M., Cooper, T.B., Arango, V., Mann, J.J., 2006. Acute Occupancy of Brain Serotonin Transporter by Sertraline as Measured by [11C]DASB and Positron Emission Tomography. Biological Psychiatry 59 (9), 821–828.

Peters, M.E., Vaidya, V., Drye, L.T., Devanand, D.P., Mintzer, J.E., Pollock, B.G., Porsteinsson, A.P., Rosenberg, P.B., Schneider, L.S., Shade, D.M., Weintraub, D., Yesavage, J., Lyketsos, C.G., Avramopoulos, D., 2016. Citalopram for the Treatment of Agitation in Alzheimer Dementia. Journal of Geriatric Psychiatry and Neurology 29 (2), 59–64.

Qiao, Z., Mardon, K., Stimson, D. H. R., Migotto, M. anne, Reutens, D. C., & Bhalla, R. (2020). Synthesis and evaluation of 6-[18F]fluoro-3-(pyridin-3-yl)-1H-indole as potential PET tracer for targeting tryptophan 2, 3-dioxygenase (TDO). *Nuclear Medicine and Biology*. https://doi.org/10.1016/j.nucmedbio.2019.12.007.

Rabinovici, G.D., Jagust, W.J., 2009. Amyloid imaging in aging and dementia: Testing the amyloid hypothesis in vivo. In *Behavioural Neurology*. https://doi.org/10.3233/BEN-2009-0232.

Rahmim, A., Cheng, J.-C., Blinder, S., Camborde, M.-L., Sossi, V., 2005. Statistical dynamic image reconstruction in state-of-the-art high-resolution PET. In *Physics in Medicine and Biology* 50 (20), 4887–4912.

Ramirez, M.J., Lai, M.K.P., Tordera, R.M., Francis, P.T., 2014. Serotonergic therapies for cognitive symptoms in alzheimer's disease: Rationale and current status. Drugs 74 (7), 729–736.

Ramos-Rodriguez JJ, Molina-Gil S, Rey-Brea R, Berrocoso E, Garcia-Alloza M. (2013) Specific serotonergic denervation affects tau pathology and cognition without altering senile plaques deposition in APP/PS1 mice. PLoS One. Nov 21;8(11): e79947. doi: 10.1371/journal.pone.0079947.

Reiman, E.M., Caselli, R.J., Yun, L.S., Chen, K., Bandy, D., Minoshima, S., Thibodeau, S. N., Osborne, D., 1996. Preclinical Evidence of Alzheimer's Disease in Persons Homozygous for the ε4 Allele for Apolipoprotein E. New England Journal of Medicine 334 (12), 752–758.

Robert, S.J., Lezoualc'h, F., 2008. Distinct functional effects of human 5-HT4 receptor isoforms on β-amyloid secretion. Neurodegenerative Diseases. https://doi.org/10.1159/000113691.

Rolls, E.T., Joliot, M., Tzourio-Mazoyer, N., 2015. Implementation of a new parcellation of the orbitofrontal cortex in the automated anatomical labeling atlas. NeuroImage 122, 1–5.

Rolls, E.T., Huang, C.-C., Lin, C.-P., Feng, J., Joliot, M., 2020. Automated anatomical labelling atlas 3. NeuroImage 206, 116189.

Rüb, U., Del Tredici, K., Schultz, C., Thal, D.R., Braak, E., Braak, H., 2000. The evolution of Alzheimer's disease-related cytoskeletal pathology in the human raphe nuclei. Neuropathology and Applied Neurobiology 26 (6), 553–567.

Rüb, U., Stratmann, K., Heinsen, H., Del Turco, D., Seidel, K., den Dunnen, W., Korf, H.-W., 2016. The Brainstem Tau Cytoskeletal Pathology of Alzheimer's Disease: A Brief Historical Overview and Description of its Anatomical Distribution Pattern. CAR 13 (10), 1178–1197.

Sackeim, H.A., 2001. The definition and meaning of treatment-resistant depression. In. Journal of Clinical Psychiatry.

Salloway, S., Sperling, R., Fox, N.C., Blennow, K., Klunk, W., Raskind, M., Sabbagh, M., Honig, L.S., Porsteinsson, A.P., Ferris, S., Reichert, M., Ketter, N., Nejadnik, B., Guenzler, V., Miloslavsky, M., Wang, D., Lu, Y., Lull, J., Tudor, I.C., Liu, E., Grundman, M., Yuen, E., Black, R., Brashear, H.R., 2014. Two phase 3 trials of Bapineuzumab in mild-to-moderate Alzheimer's disease. New England Journal of Medicine 370 (4), 322–333.

Sheline, Y.I., Snider, B.J., Beer, J.C., Seok, D., Fagan, A.M., Suckow, R.F., Lee, J.-M., Waligorska, T., Korecka, M., Aselcioglu, I., Morris, J.C., Shaw, L.M., Cirrito, J.R., 2020. Effect of escitalopram dose and treatment duration on CSF Aβ levels in healthy older adults: A controlled clinical trial. In *Neurology* 95 (19), e2658 e2665.

Simic, G., Stanic, G., Mladinov, M., Jovanov-Milosevic, N., Kostovic, I., Hof, P.R., 2009. Does Alzheimer's disease begin in the brainstem?: Annotation. In *Neuropathology and Applied Neurobiology* 35 (6), 532–554.

Smith, G.S., Barrett, F.S., Joo, J.H., Nassery, N., Savonenko, A., Sodums, D.J., Marano, C. M., Munro, C.A., Brandt, J., Kraut, M.A., Zhou, Y., Wong, D.F., Workman, C.I., 2017. Molecular imaging of serotonin degeneration in mild cognitive impairment. Neurobiology of Disease 105, 33–41.

Smith, G.S., Kuwabara, H., Gould, N.F., Nassery, N., Savonenko, A., Joo, J.H., Bigos, K.L., Kraut, M., Brasic, J., Holt, D.P., Hall, A.W., Mathews, W.B., Dannals, R.F., Nandi, A., Workman, C.I., 2021a. Molecular Imaging of the Serotonin Transporter Availability and Occupancy by Antidepressant Treatment in Late-Life Depression. Neuropharmacology 194, 108447.

Smith, G.S., Kuwabara, H., Nandi, A., Gould, N.F., Nassery, N., Savonenko, A., Joo, J.H., Kraut, M., Brasic, J., Holt, D.P., Hall, A.W., Mathews, W.B., Dannals, R.F., Avramopoulos, D., Workman, C.I., 2021c. Molecular imaging of beta-amyloid deposition in late-life depression. Neurobiology of Aging. 101, 85–93. https://doi.org/10.1016/j.neurobiolaging.2021.01.002.

Smith, M.A., Taneda, S., Richey, P.L., Miyata, S., Yan, S.D., Stern, D., Sayre, L.M., Monnier, V.M., Perry, G., 1994. Advanced Maillard reaction end products are associated with Alzheimer disease pathology. Proc. Natl. Acad. Sci. U.S.A. 91 (12), 5710–5714.

Smith, M.A., Sayre, L.M., Anderson, V.E., Harris, P.L.R., Beal, M.F., Kowall, N., Perry, G., 1998. Cytochemical demonstration of oxidative damage in Alzheimer disease by immunochemical enhancement of the carbonyl reaction with 2,4-dinitrophenylhydrazine. Journal of Histochemistry and Cytochemistry 46 (6), 731–735.

Smith, G.S., Workman, C.I., Protas, H., Su, Y., Savonenko, A., Kuwabara, H., Gould, N.F., Kraut, M., Joo, J.H., Nandi, A., Avramopoulos, D., Reiman, E.M., Chen, K., 2021b. Positron emission tomography imaging of serotonin degeneration and beta-amyloid deposition in late-life depression evaluated with multi-modal partial least squares. Translational Psychiatry. https://doi.org/10.1038/s41398-021-01539-9.

Sossi, V., De Jong, H.W.A.M., Barker, W.C., Bloomfield, P., Burbar, Z., Camborde, M.L., Comtat, C., Eriksson, L.A., Houle, S., Keator, D., Knöß, C., Krais, R., Lammertsma, A. A., Rahmim, A., Sibomana, M., Teräs, M., Thompson, C.J., Trébossen, R., Votaw, J., Wong, D.F., 2005. The second generation HRRT - A multi-centre scanner performance investigation. IEEE Nuclear Science Symposium Conference Record. https://doi.org/10.1109/NSSMIC.2005.1596770.

Steinbusch, H.W.M., Niewenhuys, R., Verhofstad, A.A.J., Van Der Kooy, D., 1981. The nucleus raphe dorsalis of the rat and its projection upon the caudatoputamen. A combined cytoarchitectonic, immunohistochemical and retrograde transport study. Journal de Physiologie.

Tajeddinn, W., Persson, T., Maioli, S., Calvo-Garrido, J., Parrado-Fernandez, C., Yoshitake, T., Kehr, J., Francis, P., Winblad, B., Höglund, K., Cedazo-Minguez, A., Aarsland, D., 2015. 5-HT1B and other related serotonergic proteins are altered in APPswe mutation. Neuroscience Letters 594, 137–143.

Truchot, L., Costes, S.N., Zimmer, L., Laurent, B., Le Bars, D., Thomas-Anterion, C., Croisile, B., Mercier, B., Hermier, M., Vighetto, A., Krolak-Salmon, P., 2007. Up-regulation of hippocampal serotonin metabolism in mild cognitive impairment. Neurology 69 (10), 1012–1017.

Tzourio-Mazoyer, N., Landeau, B., Papathanassiou, D., Crivello, F., Etard, O., Delcroix, N., Mazoyer, B., Joliot, M., 2002. Automated anatomical labeling of activations in SPM using a macroscopic anatomical parcellation of the MNI MRI single-subject brain. NeuroImage 15 (1), 273–289.

Varnäs, K., Halldin, C., Hall, H., 2004. Autoradiographic distribution of serotonin transporters and receptor subtypes in human brain. Human Brain Mapping 22 (3), 246–260.

Villeneuve, S., Rabinovici, G.D., Cohn-Sheehy, B.I., Madison, C., Ayakta, N., Ghosh, P.M., La Joie, R., Arthur-Bentil, S.K., Vogel, J.W., Marks, S.M., Lehmann, M., Rosen, H.J., Reed, B., Olichney, J., Boxer, A.L., Miller, B.L., Borys, E., Jin, L.-W., Huang, E.J., Grinberg, L.T., DeCarli, C., Seeley, W.W., Jagust, W., 2015. Existing Pittsburgh Compound-B positron emission tomography thresholds are too high: Statistical and pathological evaluation. Brain 138 (7), 2020–2033.

Wilson, A.A., Ginovart, N., Hussey, D., Meyer, J., Houle, S., 2002. In vitro and in vivo characterisation of [11C]-DASB: A probe for in vivo measurements of the serotonin transporter by positron emission tomography. Nuclear Medicine and Biology 29 (5), 509–515.

Wilson, A.A., Garcia, A., Chestakova, A., Kung, H., Houle, S., 2004. A rapid one-step radiosynthesis of the β-amyloid imaging radiotracer N-methyl-[11C]2-(4′-methylaminophenyl)-6-hydroxybenzothiazole ([11C]-6-OH-BTA-1). Journal of Labelled Compounds and Radiopharmaceuticals 47 (10), 679–682.

Wilson, A.A., Sadovski, O., Nobrega, J.N., Raymond, R.J., Bambico, F.R., Nashed, M.G., Garcia, A., Bloomfield, P.M., Houle, S., Mizrahi, R., Tong, J., 2017. Evaluation of a novel radiotracer for positron emission tomography imaging of reactive oxygen species in the central nervous system. Nuclear Medicine and Biology 53, 14–20. https://doi.org/10.1016/j.nucmedbio.2017.05.011.

Wu, W., Nicolazzo, J.A., Wen, L.i., Chung, R., Stankovic, R., Bao, S.S., Lim, C.K., Brew, B. J., Cullen, K.M., Guillemin, G.J., Adlard, P.A., 2013. Expression of Tryptophan 2,3-Dioxygenase and Production of Kynurenine Pathway Metabolites in Triple Transgenic Mice and Human Alzheimer's Disease Brain. PLoS ONE 8 (4), e59749.